International Journal of Geosynthetics and Ground Engineering (2021) 7:57
https://doi.org/10.1007/s40891-021-00304-8

ORIGINAL PAPER

A Numerical Study on the Role of EPS Geofoam in Reducing Earth Pressure on Retaining Structures Under Dynamic Loading

Muhammad Imran Khan[1,2] · **Mohamed A. Meguid**[1]

Received: 8 April 2021 / Accepted: 27 July 2021

Abstract
The magnitude of lateral earth pressure plays an important role in the analysis and design of earth retaining structures. Expanded polystyrene (EPS) geofoam panels have been successfully used in reducing lateral thrust on walls under static loading condition. The presence of geofoam panels between a rigid wall and the backfill soil allows for controlled deformation to develop, which leads to the mobilization of soil shear strength. When subjected to dynamic loading, the magnitude of earth pressure acting on a rigid wall can become significantly larger. In this study, a finite element model is developed to investigate the effectiveness of installing geofoam buffer behind a rigid retaining wall on the seismic lateral thrust induced by the backfill material. A parametric study was then conducted to investigate the effect of geofoam density, relative thickness of the geofoam with respect to the wall height and the friction angle of the backfill soil on the effectiveness of this technique to reduce the impact of seismic events on the stability of the wall. Results showed that provision of geofoam behind rigid non-yielding retaining wall can provide 10–40% reduction in seismic thrust depending on the geofoam density, relative thickness and frictional properties of the backfill soil.

Keywords Lateral earth pressure · Rigid retaining wall · EPS geofoam · Seismic buffer · Isolation efficiency

Introduction

Expanded polystyrene (EPS) geofoam has a long history with successful applications in the field of transportation and geotechnical engineering. The generic term "geofoam" was first introduced by Horvath [1] for rigid plastic foam type materials used in geotechnical applications. Later, the term "geofoam" was expanded to include any cellular material manufactured by an expansion process [2]. These synthetic materials are now part of the geosynthetic family as proposed by Horvath [3].

The early use of EPS geofoam in geotechnical engineering started in 1960s. The Norwegian geotechnical engineers used EPS geofoam for thermal insulation in roads [4] and in lightweight road embankments constructed over soft soils [5]. Due to its lightweight nature ($\rho = 12$–39 kg/m^3) and relatively high strength, EPS geofoam has been used in several geotechnical applications, including, slope stabilization [6–10], subbase fill material [11–14], embankments [15–19], earth retaining structures [20], bridge approaches and abutments [21–25], buried pipes [26–28] and seismic buffer [29–33].

Retaining structures (e.g. cantilever walls, basement walls and bridge abutments) are integral components of many infrastructure projects. Retaining walls can be classified as either "non-yielding" or "yielding" depending on whether horizontal displacement and wall deformation are permitted [34].

Past experience showed that retaining walls may be vulnerable to severe damage under excess dynamic forces induced during an earthquake. Several post-earthquake studies revealed that large displacements can lead to excessive wall deformation and possibly failure [35]. Therefore, in seismically active areas, a retaining structure must be designed to resist both static and dynamic earth pressures. The current USA and Canadian building codes emphasise the use of an increased earthquake return period in the

✉ Mohamed A. Meguid
mohamed.meguid@mcgill.ca

Muhammad Imran Khan
muhammad.khan14@mail.mcgill.ca

1 Department of Civil Engineering, McGill University, Montreal, QC H3A 0C3, Canada

2 Department of Civil Engineering, University of Engineering and Technology, Lahore, Pakistan

design of civil engineering structures in seismically active regions [36, 37], which results in higher design loads on earth retaining structures. Therefore, both geotechnical and structural engineers are interested in developing new methodologies to attenuate larger seismic loads on earth retaining structures, which in turn leads to an economical and safe design. EPS geofoam has proven its advantage as light weight backfill that can resist both lateral and vertical pressures associated with geotechnical engineering structures. To suit the wide range of applications, material density and the corresponding stress–strain behavior of geofoam can be controlled during the manufacturing process.

Compressible geofoam inclusion placed behind a rigid retaining wall has been suggested to attenuate dynamic earth forces by allowing controlled yielding of the backfill material [38–45]. The idea of using EPS geofoam as compressible inclusion is not new. Researchers have shown that static lateral loads acting on retaining walls can be reduced by placing EPS geofoam blocks between the wall and the backfill soil without increasing the wall stiffness [46–53]. The work of Khan and Meguid [54] focused on wall response under static loading, however, during an earthquake event, compressible geofoam panels allow for the lateral expansion of the backfill soil (controlled yielding) by absorbing significant portion of the seismic lateral thrust while the remaining thrust is transferred safely to the retaining structure. Lateral expansion of the backfill also helps in the mobilization of soil shear strength, which brings the surrounding soil to active state. This technique can be applied to both new and existing structures.

In a case study, Inglis et al. [55] reported the first use of geofoam as seismic buffer in Vancouver, Canada. Vertical EPS panels (450–610 mm in thickness) were placed behind three rigid basement walls to reduce dynamic lateral earth pressure during an earthquake (see Fig. 1). Pseudo-static analysis [56], pseudo-dynamic analysis [57–59] and dynamic analysis [60] were performed to compute the seismic earth pressures on the walls. Results from these analyses showed that the presence of about 1 m thick EPS geofoam inclusion between the rigid retaining wall and the backfill can reduce the lateral seismic earth pressure by about 50% in comparison to rigid retaining wall with no geofoam buffer.

According to Inglis et al. [55] a good buffer material should: (a) be strong and rigid enough to withstand static soil forces with small deformations and creep but at the same time should also be able to resist the possible dynamic forces without causing failure; (b) be inert and should not deteriorate due to water, chemical attack, aging, etc.; (c) be economical in comparison to the cost of the structure. A summary of some of the experimental and numerical studies performed to examine the role of geofoam in attenuating seismic earth pressure on retaining walls is given below.

Experimental Studies

Bathurst et al. [42] presented a proof of concept for the application of geofoam as seismic buffer behind rigid retaining walls using 1 g shaking table. Results showed that low density geofoam can achieve up to 40% reduction in pressure (at a peak base acceleration of 0.8 g) while higher density geofoam achieved about 15% reduction in earthquake load compared to the control test. Hazarika et al. [40, 61] conducted reduced-scale shaking table tests on a 0.7 m high retaining wall models with different buffer thickness. The buffer used in this study was a sponge type material with density of 22 kg/m^3. Results showed that provision of EPS geofoam layer between the wall and backfill soil can reduce the peak lateral load on the wall by 30–60%.

Dasaka et al. [44] performed shaking table tests on a reduced-scale gravity retaining wall subjected to both surcharge and seismic loading. It was found that provision of ESP geofoam can reduce the maximum seismic thrust on the wall by about 28%. In a similar study, Dave et al. [62] found that retaining walls with hinged boundary showed a hydrostatic seismic pressure distribution while fixed walls showed a curvilinear seismic pressure distribution. Ertugrul et al. [45, 63, 64] found that low density geofoam can reduce pressure by up to 50% of the dynamic thrust acting on the wall.

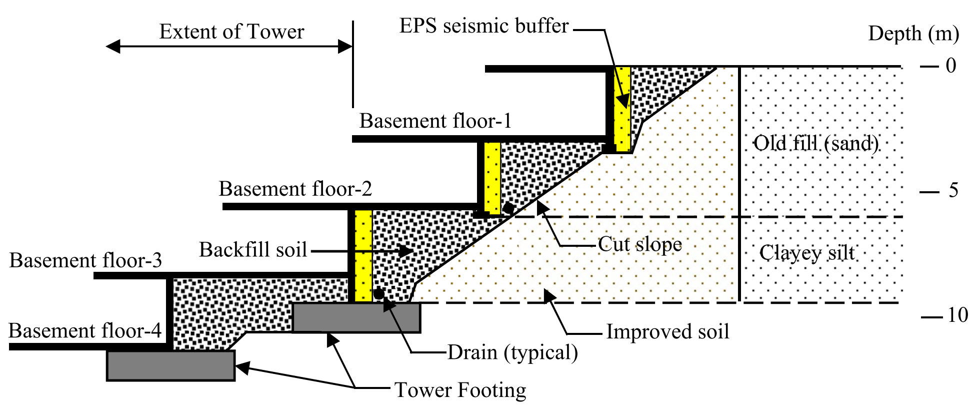

Fig. 1 Using geofoam blocks as seismic buffer behind basement walls in Vancouver, Canada (modified from [55])

Athanasopoulos-Zekkos et al. [43] performed centrifuge tests on 4 m high rigid retaining wall models and confirmed the reduction in seismic earth pressure as a result of the controlled yielding of the backfill associated with the compression of the geofoam inclusion. A summary of the reported shaking table tests, comparing the wall geometries, boundary conditions and the measured results, is provided in Table 1.

Numerical Studies

Inglis et al. [55] modelled a 10 m high wall with geofoam seismic buffer under a simulated earthquake loading and showed that the provision of EPS as seismic buffer reduced the peak lateral stress on the wall by up to 50%. Pelekis et al. [65] analyzed cantilever retaining walls subjected to base acceleration that ranges between 0.1 g and 0.5 g and found that, depending on the thickness and stiffness of the geofoam, a significant reduction in seismic earth pressure can be achieved. Armstrong and Alfaro [66] modeled a 10 m high wall under peak acceleration of 1.9 g. It was found that EPS blocks used as seismic buffer reduced 25% of the passive seismic thrust while a minimal reduction in active seismic thrust was calculated. Zarnani et al. [67–69] and Zarnani and Bathurst [70] found that geofoam stiffness plays a significant role in the design of these composite systems. Athanasopoulos et al. [71] numerically evaluated the response of retaining walls built with geofoam inclusion subjected to harmonic base excitations. It was found that geofoam density, thickness, wall height and wall flexibility affect the efficiency of the geofoam as a seismic buffer. Zekkos et al. [72] showed that for non-yielding walls, isolation efficiency increases with the increase in inclusion thickness. Wang et al. [73] and Wang and Bathurst [74] found that lower density geofoam can absorb a significant amount of energy during earthquake. A summary of some of the reported numerical studies and the details of the investigated models is presented in Table 2.

Scope and Objective

Studies dedicated to investigate the role of EPS geofoam and backfill properties on the seismic earth pressure on retaining walls are scarce in the literature. In this study, a two-dimensional finite element model is developed and validated using experimental data. The model is then used to perform a parametric study to investigate the effect of geofoam density, relative thickness of the geofoam with respect to the wall height and the friction angle of the backfill soil on reducing the seismic lateral earth pressure acting on retaining walls. Normalized charts that help to evaluate the isolation efficiency of the system are presented.

Description of the Physical Model

In this study, 1 g shaking table tests [42] that have been reported for a small scale rigid non-yielding retaining wall with geofoam inclusion were used as a basis for the current analysis. Wall models were built and tested in a rectangular container (2.5 m × 1.4 m × 1.3 m) attached to a shaking table platform (2.7 m × 2.7 m in plan area) as shown in Fig. 2. A 6 mm thick rigid wall was placed on linear bearings at the front of the rectangular container, which could be moved to place 0.15 m thick EPS geofoam between the wall and backfill soil. Dry synthetic olivine sand was used as backfill material. Blocks of EPS geofoam having density of 16 kg/m^3 were placed between the wall and backfill. Properties of the soil and the geofoam are provided in Table 3.

A 5 Hz frequency variable-amplitude sinusoidal base acceleration record (with peak accelerations 0.8 g) as shown in Fig. 3a, was applied as horizontal base excitation. The acceleration amplitude was increased in increments of 0.05 g and each increment was kept for 5 s. A 2-s accelerogram window at an amplitude step is shown in Fig. 3b. According to the scaling rules proposed by Iai [75], a 5 Hz frequency (i.e. 0.2 s period) corresponds to 2 Hz frequency (i.e. 0.5 s period) at 1/6 prototype model scale. This simple stepped-amplitude sinusoidal base acceleration record is generally more aggressive than an actual earthquake record with the

Table 1 Shaking table test results

Property	Bathurst et al. [42]	Hazarika et al. [40, 60]	Dasaka et al. [44]	Ertugrul et al. [45, 63, 64]
Wall height H (mm)	1000	700	700	700
Relative thickness t/H	0.15	0.08	0.125	0.14
Wall type	Rigid	Rigid	Rigid	Flexible
Inclusion material	EPS geofoam	Sponge	EPS geofoam	EPS geofoam
Acceleration, a (g)	0.7	0.8	0.7	0.7
Reduction (%)	40	30–60	28	50

Table 2 Summary of previous numerical studies

Reference	Approach/software	Assumptions/models
Inglis et al. [55]	FDM/FLAC	*Soil*: Mohr Coulomb *EPS geofoam*: Double yield constituency model
Pelekis et al. [65]	FEM/FLUSH PLUS	*Soil & EPS geofoam*: Viscoelastic materials with strain-dependent values of shear modulus and damping ratio
Armstrong et al. [66]	FDM/FLAC	*Soil*: Mohr Coulomb *EPS geofoam*: Hyperbolic model
Zarnani et al. [67–69]	FDM/FLAC	*Soil*: Mohr Coulomb *EPS geofoam*: Linear elastic–plastic
Athanasopoulos et al. [71]	FEM/PLAXIS	*Soil*: Non-linear *EPS geofoam*: Non-linear
Zekkos et al. [72]	FEM/PLAXIS	*Soil*: Elasto-plastic *EPS geofoam*: Linear elastic
Wang et al. [73]	FDM/FLAC	*Soil*: Mohr Coulomb *EPS geofoam*: Linear elastic
Wang and Bathurst [74]	FEM/ABAQUS	*Soil*: Mohr Coulomb *EPS geofoam*: Linear elastic–plastic
Khan and Meguid (present study)	FEM/PLAXIS	*Soil*: Hardening soil *EPS geofoam*: Linear elastic

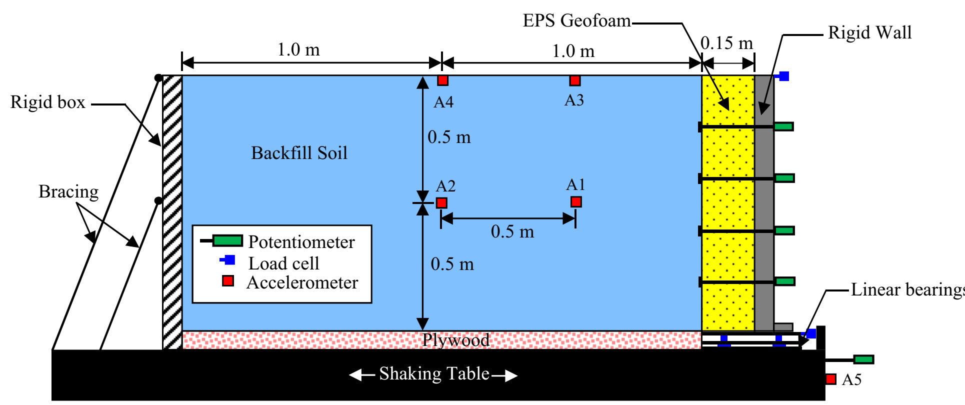

Fig. 2 Description of the shaking table test setup (modified from [42])

Table 3 Properties of the backfill and EPS geofoam materials used in the model validation

Property	Backfill soil	EPS geofoam
Unit weight, γ (kN/m^3)	15.7	0.15
Young's modulus, E (kN/m^2)	15,200	4700
Poisson's ratio, υ	0.33	0.09
Cohesion c' (kN/m^2)	0	–
Peak friction angle ϕ_p (degrees)	51	–
Residual friction angle ϕ_r (degrees)	46	–
Dilatancy angle Ψ' (degrees)	15	–
Specific gravity	2.88	–
c_c (coefficient of curvature)	1.27	–
c_u (coefficient of uniformity)	2.5	–
Percent finer than #200 sieve (%)	<3	–

same predominant frequency and amplitude [76, 77]. Moreover, a stepped record is known to simplify the interpretation of seismic response, and is, therefore, adopted in this study.

Numerical Analysis

Model Validation

The numerical simulations were performed using the dynamic module in the finite element software PLAXIS [78]. Two-dimensional plane strain models were developed to simulate the dynamic response of the wall. The height and width of numerical models and thickness of EPS geofoam were selected to match the dimensions used in the physical

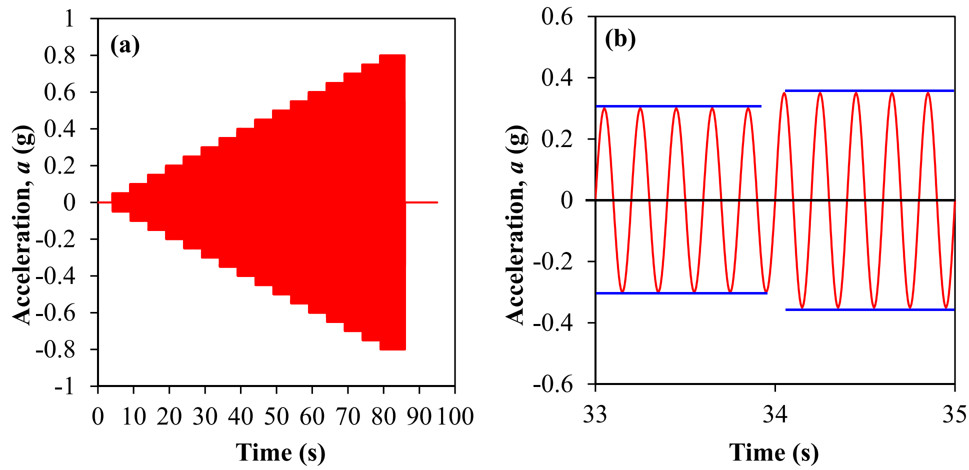

Fig. 3 **a** Input horizontal base accelerogram; **b** Two-second accelerogram window at amplitude step (modified from [42])

models. Several mesh sizes, and time increments were tested to find a suitable mesh size, time increment and max step that maintain a balance between accuracy and computing cost. The used FE mesh, geometry and boundary conditions is shown in Fig. 4. The retaining wall and the back of the box were modelled using plate elements, whereas the backfill material was modelled using 15-node triangular plane strain elements.

Boundary conditions were set such that displacements along the vertical boundaries were restrained in the *x*-direction (smooth rigid) during the generation of the initial stress state and released during the dynamic loading phase. Displacements along the bottom boundary were fixed in both the *x*- and *y*-directions (rough rigid) during the initial phase and released in the *x*-direction during dynamic loading phase. Interfaces between the wall-backfill, wall-EPS and EPS-backfill were also specified. The backfill was modelled using the Hardening Soil (HS) model with Rayleigh damping. The HS model is an elasto-plastic second-order hyperbolic isotropic-hardening model developed by Schanz et al. [79]. The EPS geofoam was modelled as linear elastic material. This is considered to be appropriate given the low strain levels reported in the experiments. The material properties of backfill soil and EPS geofoam are given in Table 3.

The steps taken in creating the model can be summarized as follows: (1) simulating the box, retaining wall, backfill soil and EPS geofoam in an initial step; (2) the application of stepped-amplitude sinusoidal input excitation at the base with a peak acceleration of 0.8 g.

The numerically calculated and measured results are shown in Fig. 5a, b before and after the geofoam installation. As the time increases from 0 to about 86 s, the acceleration amplitude is found to increase from 0 to 0.8 g, which significantly increases the peak horizontal force on the wall from about 3.5 kN/m to about 15 kN/m. After the installation of the geofoam panels behind the wall, the rate of change in peak horizontal force is found to decrease where a maximum horizontal force of about 12 kN/m is reached after 86 s have elapsed.

An overall agreement in the rate of change in peak horizontal force with time was found between the calculated and measured responses. It is worth noting that some differences

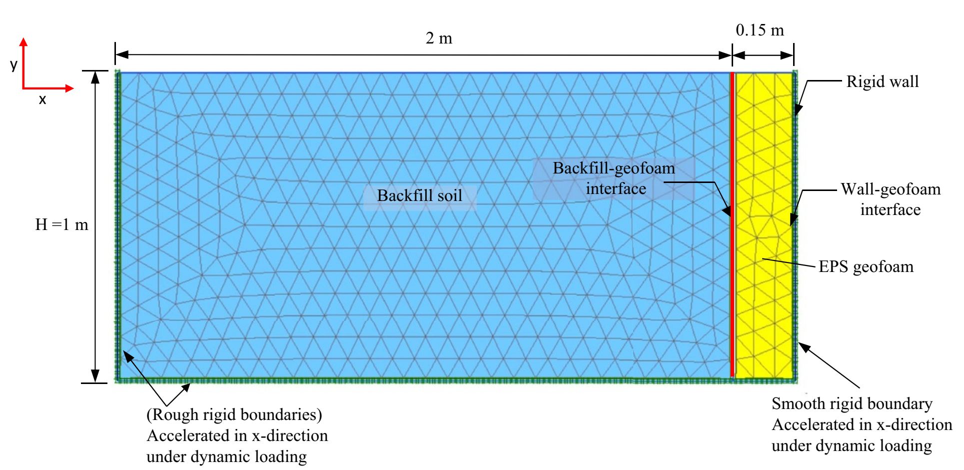

Fig. 4 Finite element mesh of a retaining wall with geofoam inclusion

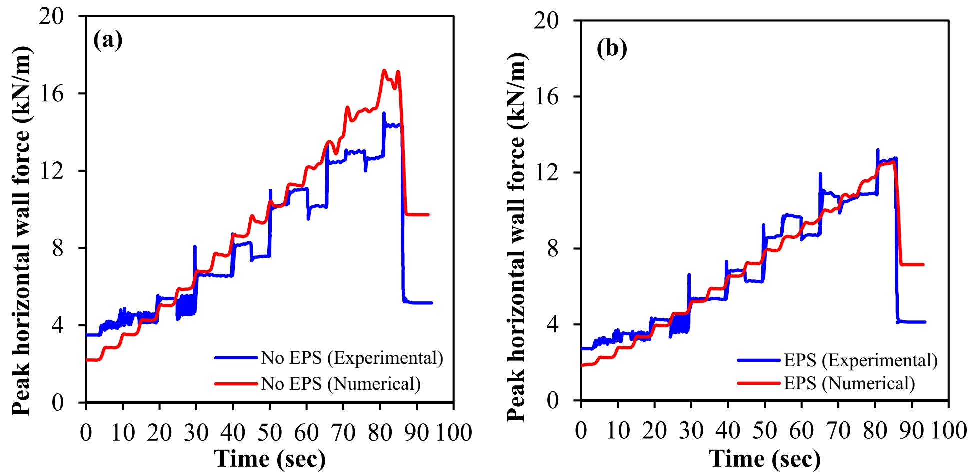

Fig. 5 Model validation. **a** Wall without geofoam inclusion. **b** Wall with geofoam inclusion

in horizontal forces were observed in both models (Fig. 5a, b), particularly within the first 15 s, where the calculated values were lower than those measured in the experiments. This is explained by the locked-in stresses induced by the compaction process reported in the experiment, which could not be fully simulated by the numerical model. That effect was found to be less pronounced for the case involving geofoam (Fig. 5b).

Figure 6 shows the calculated accelerations at the four monitored locations A1 through A4 within the experiment (see Fig. 2). It can be seen that the dominant frequency in the backfill soil is consistently 5 Hz, which agrees well with that of the frequency of the input signal. This confirms that the developed model is able to reasonably simulate the conditions in the experiment and could be used to evaluate the role of the critical parameters in the overall performance of the system.

Parametric Analysis

A parametric study was conducted to examine the effect of geofoam density and relative thickness as well as the friction angle of the backfill material on the changes in dynamic lateral force acting on the wall. The model illustrates in Fig. 4 is used as the basis for this study. The backfill material was modelled using Hardening Soil (HS) model with Rayleigh damping. Four different backfill materials with friction angles that range from 30° to 45° were considered in the parametric study. Four different geofoam densities representing EPS15, EPS22, EPS29 and EPS39 with three different EPS thickness "*t*" to wall height "*H*" ratios, *t/H*, of 0.1, 0.2 and 0.3 were considered. The stress–strain relationships for the geofoam materials based on uniaxial compression tests are shown in Fig. 7. For geofoam densities of 15 (EPS15), 22 (EPS22), 29 (EPS29) and 39 (EPS39) kg/m^3, the reported compressive strength values at 1% strain are found to be 45, 70, 94 and 192 kPa, respectively. Therefore, given the expected range of lateral pressure (2–19 kPa) acting on the wall, the geofoam panel is assumed to behave as linear elastic material. This was further verified numerically by examining the strains developing in the geofoam in the various steps of the analysis, which was found to be consistently below 1%. The soil and geofoam parameters used in the analysis are summarized in Table 4.

The boundary conditions, input excitation and time used in all simulations are consistent with those used in the

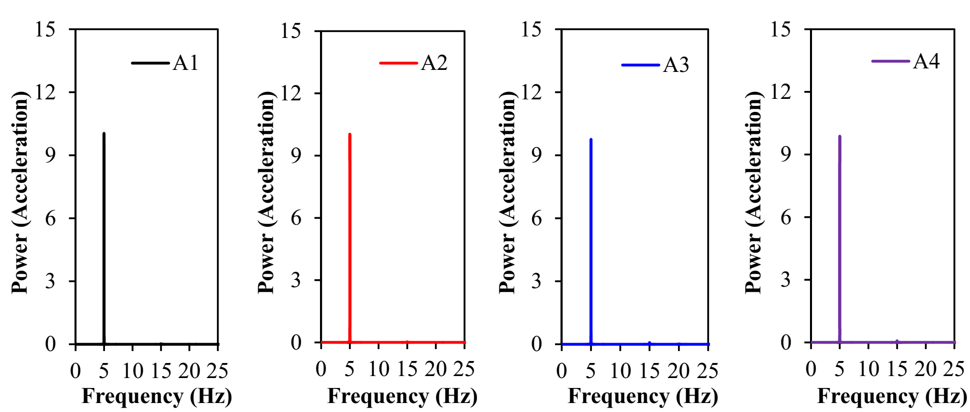

Fig. 6 Calculated acceleration at locations A1, A2, A3 and A4

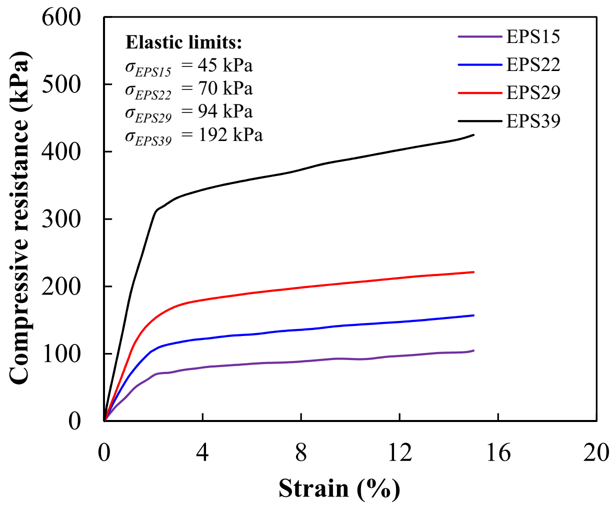

Fig. 7 Stress–strain relationships of the different geofoam materials

validated model reported in Fig. 3. Before conducting the parametric study, a convergence analysis was performed using different mesh sizes covering different cases involving geofoam panels with relative thickness of 0.1, 0.2 and 0.3 with respect to the wall height. In total, 52 simulations were run, 4 without EPS geofoam and 48 with EPS geofoam to study the role of EPS geofoam in reducing seismic earth pressure behind rigid non-yielding retaining wall.

Results and Discussion

The results of the numerical study are presented by comparing the computed peak wall force–time response before and after adding geofoam blocks of different thicknesses and density behind the wall. The peak incremental dynamic force or lateral thrust, ΔT, was computed by integrating the peak dynamic horizontal earth pressure distribution along the wall height at a particular time step. The computed peak wall force–time responses are presented in Fig. 8a–h for backfill material with friction angles of 30° and 35° and in Fig. 9a–h for backfill material with friction angles of 40° and 45°. Four EPS geofoam densities, namely, 15, 22, 29 and 39 kg/m^3 and three relative geofoam thicknesses ($t/H = 0.1$, 0.2 and 0.3) are considered in this study. The effect of the various parameters on the wall response are presented in the following sections.

Benchmark case (no geofoam)

In Figs. 8a–h and 9a–h, the analysis of the benchmark cases (No EPS line) shows the value of peak horizontal force acting on the wall for a range of backfill soil materials. The peak force at time $t = 0$, corresponds to static condition and the peak wall force at time $t \neq 0$, corresponds to dynamic condition. For all four backfill soils, it can be seen that as the time increases from 0 to 86 s, acceleration amplitude also increases from 0 to 0.8 g which causes significant increase in the horizontal force acting on the wall. It is also found that the increase in friction angle from 30° to 45° results in a decrease in the static lateral thrust from about 3.9 to 2.3 kN/m, whereas the seismic lateral thrust increases from about 15.7 to 17.3 kN/m.

Effect of Geofoam Density

It is evident from Figs. 8a–h and 9a–h that for a given backfill material and geofoam thickness, the decrease in geofoam density (stiffness) causes reduction in the seismic peak force on the wall. For example, for backfill soil with a friction angle of 40° and $t/H = 0.3$, the peak seismic wall forces increased from about 10.6 to 12.7 kN/m as the density of the installed geofoam increased from 15 to 39 kg/m^3. This is due to the fact that softer geofoam has the ability to absorb more energy under the same applied dynamic lateral thrust, which in turns can allow for more movement to develop and consequently less pressure on the wall. Therefore, low density geofoam blocks seem to be more effective in this application as compared to high density geofoam as long as the generated strains are within the acceptable limits.

Table 4 Material properties of soil and EPS geofoam (present study)

Property	Backfill soil	EPS15	EPS22	EPS29	EPS39
Material model	Hardening soil	Linear elastic	Linear elastic	Linear elastic	Linear elastic
Unit weight, γ (kN/m^3)	15.7	0.15	0.22	0.29	0.39
Young's modulus, E (kN/m^2)	15,330	4200	6910	10,000	178,000
Poisson's ratio, υ	0.33	0.11	0.12	0.13	0.15
Cohesion c' (kN/m^2)	0	–	–	–	–
Friction angle ϕ' (degrees)	30°–45°	–	–	–	–
Dilatancy angle Ψ' (degrees)	15	–	–	–	–
K_o determination	0.292–0.50	–	–	–	–

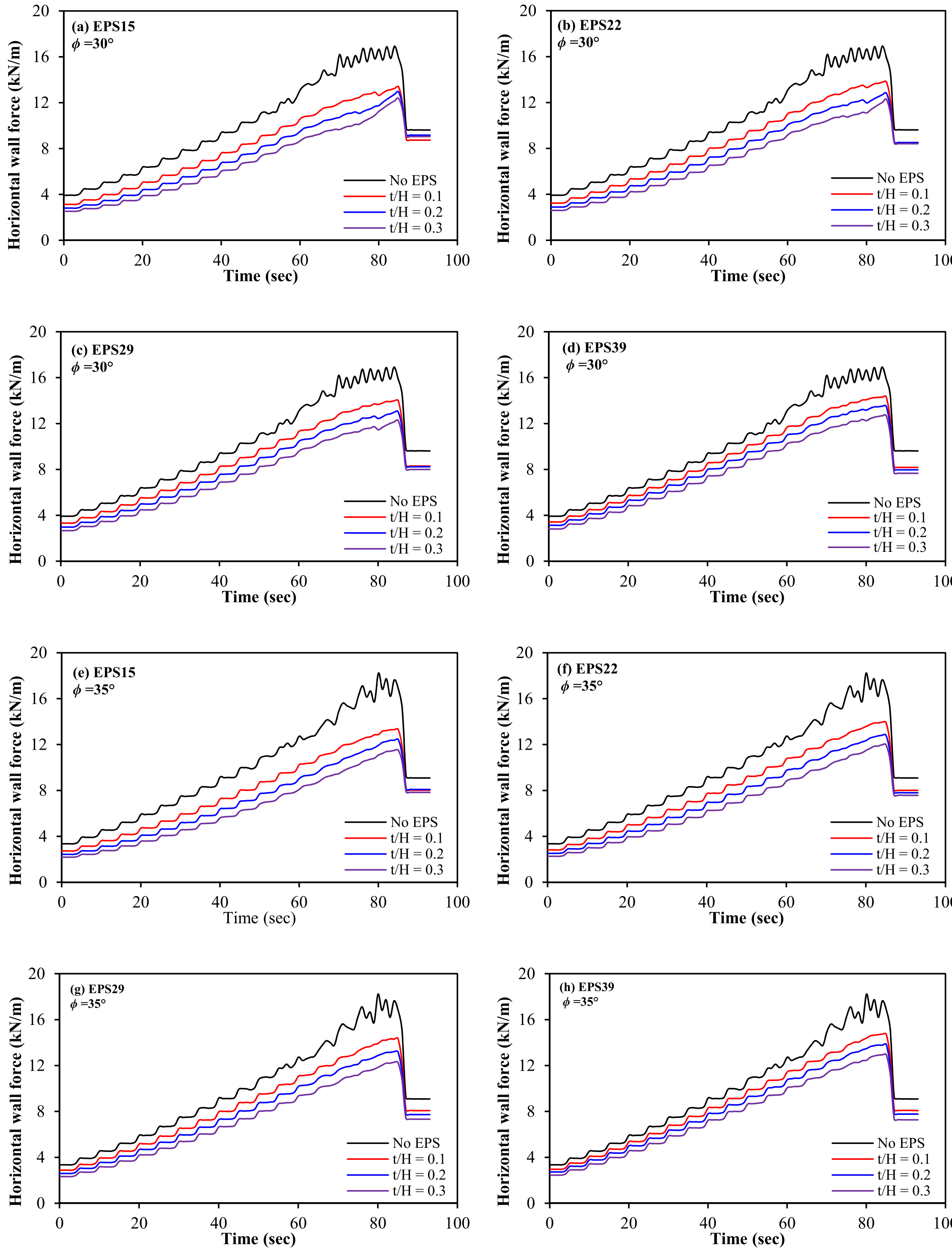

Fig. 8 Horizontal wall force for different geofoam densities, thicknesses and backfill properties

Effect of Geofoam Thickness

Inspection of Figs. 8a–h and 9a–h reveals that for a given backfill and geofoam density, the increase in the relative thickness of the geofoam (*t/H*) causes reduction in the seismic peak force acting on the wall. For example, for a backfill soil with a friction angle of 40° and geofoam density 15 kg/m^3 (EPS15), the peak seismic wall forces decreased from 14.30 to 10.62 kN/m as the relative thickness of EPS geofoam (*t/H*) was varied from 0.1 to 0.3.

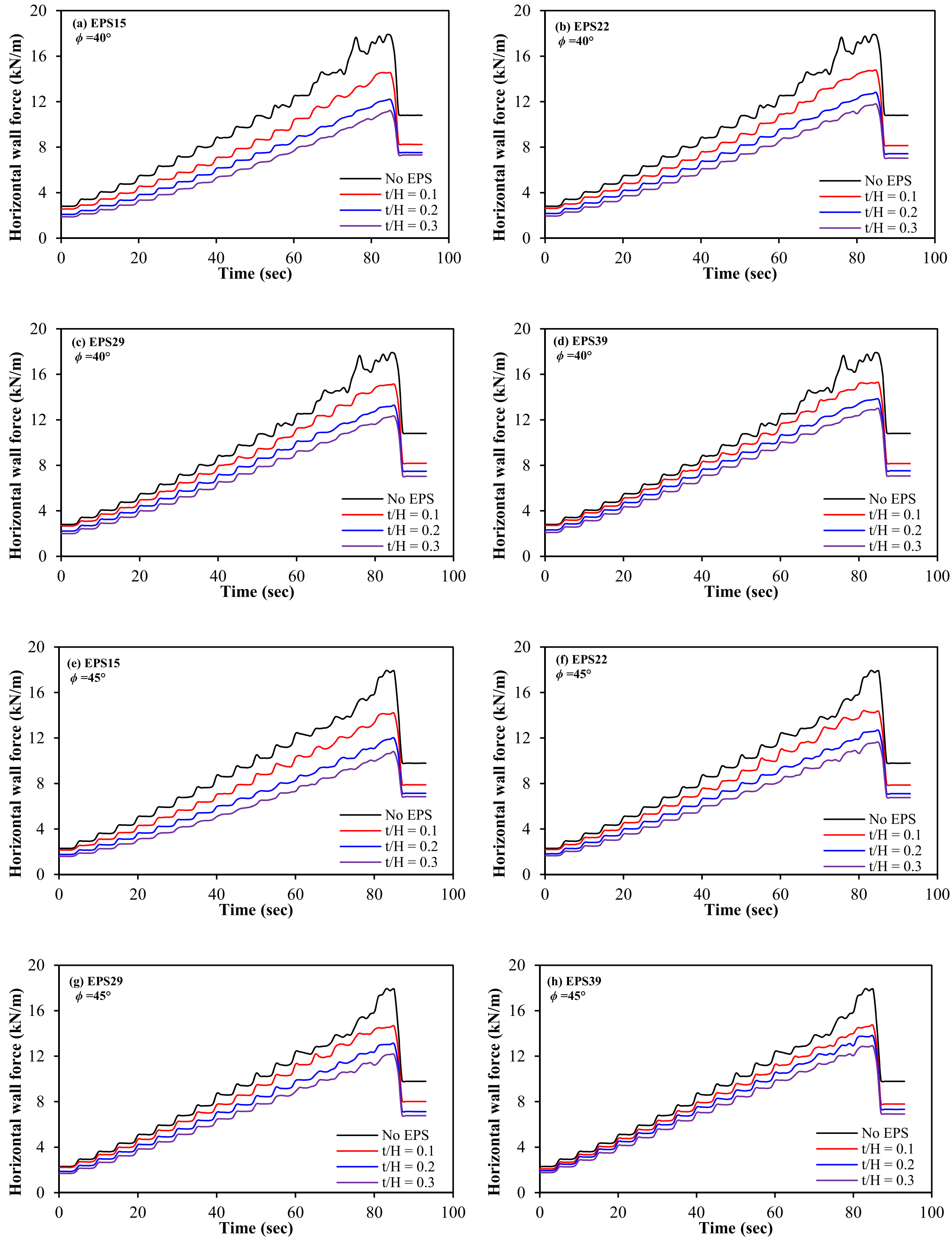

Fig. 9 Horizontal wall force for different geofoam densities, thicknesses and backfill properties

This is consistent with the fact that thick geofoam blocks compress more as compared to thin geofoam of same density, which results in more compression and more energy is absorbed under the same applied force.

Effect of Friction Angle of the Backfill Soil

The frictional properties of the backfill soil is known to be a contributing factor that can affect the magnitude of both the

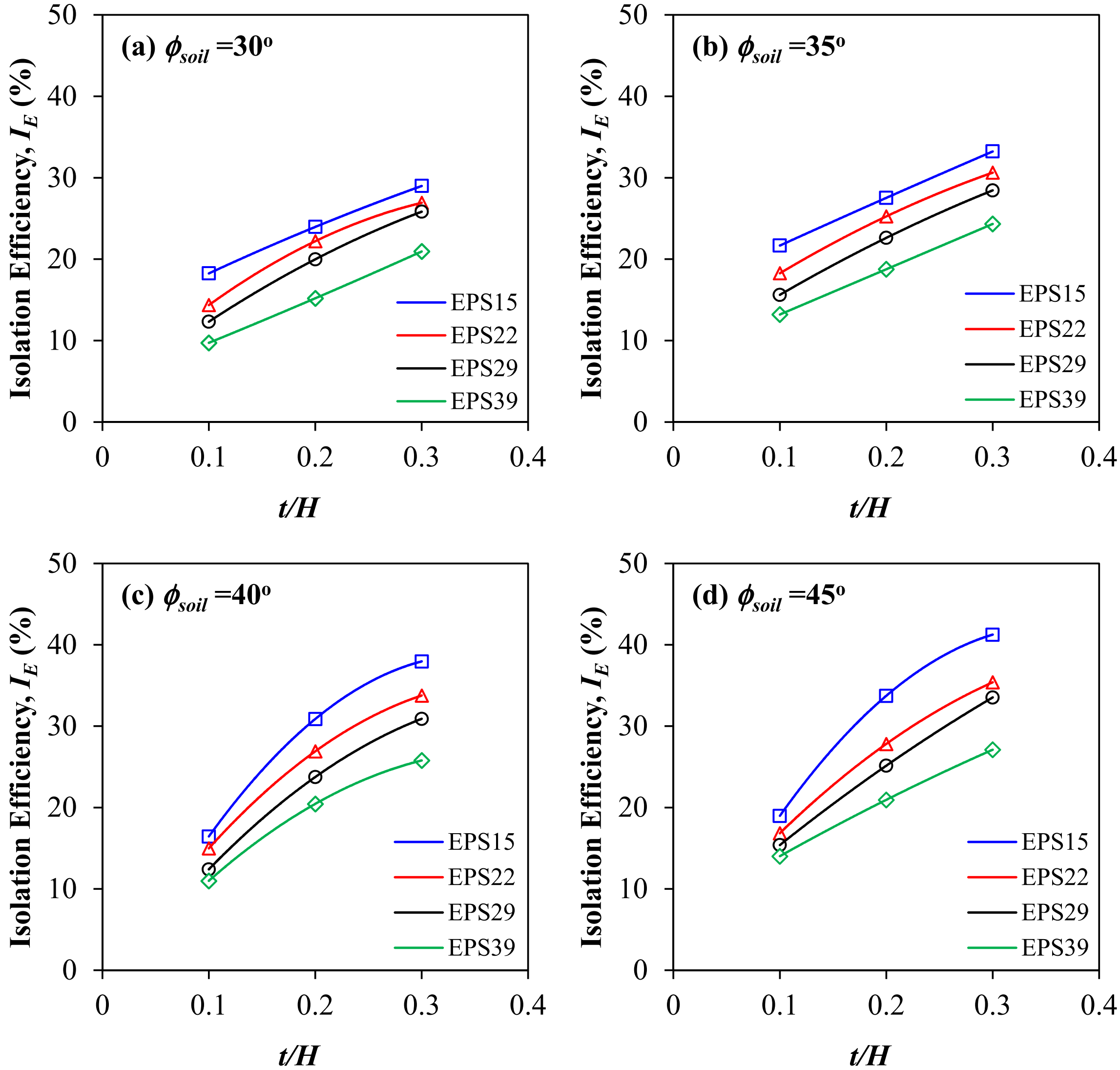

Fig. 10 Isolation efficiency vs relative geofoam thickness for: **a** $\phi = 30°$, **b** $\phi = 35°$, **c** $\phi = 40°$, **d** $\phi = 45°$

Table 5 Comparison of isolation efficiency with previous research

Reference	Relative thickness of EPS geofoam (%)	Isolation efficiency, I_E (%)
Inglis et al. [55]	4.5–6.1	50
Pelekis et al. [65]	1–14	> 50
Armstrong et al. [66]	2.5–10	25
Zarnani et al. [67–69]	2.5–40	> 50
Athanasopoulos et al. [71]	2.5–30	> 50
Zekkos et al. [72]	1.5–10	50
Wang et al. [73]	15	40
Wang and Bathurst [74]	15	45
Khan and Meguid (this study)	10–30	40

static and seismic earth pressures. It is observed that for a given geofoam thickness and density, as the friction angle of the backfill soil increases from 30° to 45°, the static lateral thrust decreased from about 3.9 to 2.3 kN/m as shown in Fig. 8a–h. This is consistent with the fact that earth pressure coefficient decreases with the increase in friction angle of the backfill soil. In contrast, for a given geofoam thickness and density, as the friction angle of the backfill soil increases from 30° to 45°, the seismic lateral thrust increased from 15.7 to 17.3 kN/m as shown in Fig. 9a–h). This is attributed to the response of EPS geofoam panel under dynamic loading. For example, for EPS15 with *t/H* ratio of 0.2, the peak seismic wall forces slightly changed from about 11.4 kN/m to a maximum of 12 kN/m as the friction angle (ϕ) of backfill soil changed from 30° to 45°. This means that, under dynamic loading, walls with geofoam inclusion perform

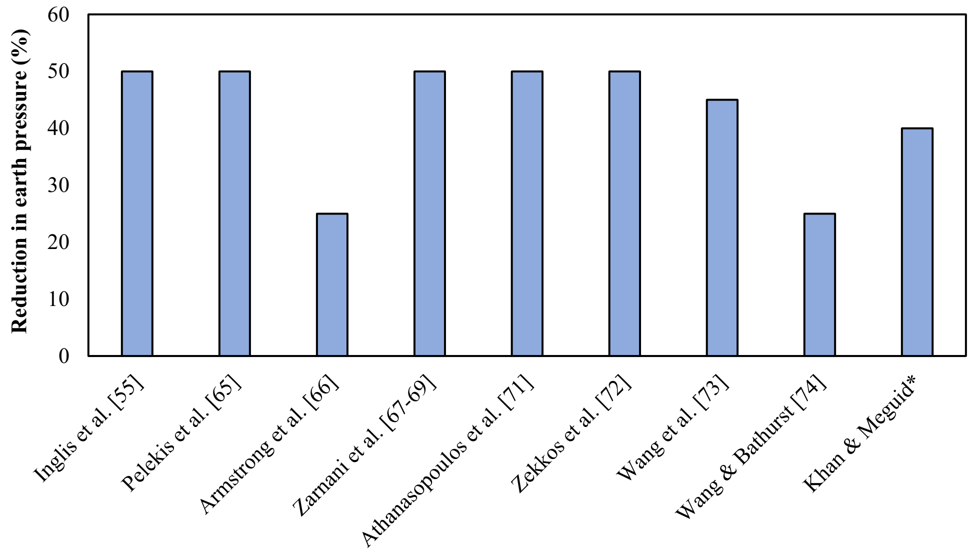

Fig. 11 Comparison of achieved pressure reduction with previous studies

better as the geofoam panel absorbs more pressure, particularly when used with backfill soil of lower frictional angle.

Isolation Efficiency (I_E)

The performance of EPS geofoam behind rigid retaining walls under seismic conditions can also be evaluated by computing the Isolation Efficiency (I_E), which is "the ratio of the difference between the peak lateral seismic thrust for benchmark (no geofoam) case (T_o) and the case where geofoam is installed (T_{EPS}) to the peak lateral seismic thrust for the benchmark case (T_o)" as expressed below:

$$I_E = \frac{T_o - T_{EPS}}{T_o} \times 100.$$

Figure 10a–d shows the influence of backfill frictional properties, geofoam densities and relative thicknesses on the isolation efficiency (I_E). Isolation efficiency is directly related to the relative thickness of the geofoam and inversely related to geofoam density. It is observed that for a given backfill properties and geofoam density, using thinner geofoam panel ($t/H = 0.1$) results in lower isolation efficiency values as compared to the case of thick geofoam panel ($t/H = 0.3$). To confirm the validity of the calculated isolation efficiency values, the results are compared with the previously published results for the case of rigid non-yielding walls as presented in Table 5. For the cases where the reported relative thickness of the geofoam panel is 15% of the wall height [73, 74], the isolation efficiency values were 40% and 45%, respectively. This is consistent with the results of this study where an isolation efficiency of about 40% is calculated for the evaluated range of wall thickness (10–30%). The percentage reduction in pressure is also compared with that reported in previous studies and the results are presented in Fig. 11. For the investigated range of geofoam thickness, the calculated responses are found to be generally consistent with those reported by researchers, which confirms the effectiveness of geofoam panels in reducing seismic earth pressure on retaining walls.

Conclusions

In this study, a numerical model is developed to study the effect of geofoam inclusion on the seismic earth pressure acting on rigid retaining walls. The developed numerical model was first validated using experimental data obtained using shaking table tests. A parametric study was then conducted to investigate the effectiveness of EPS geofoam density, relative thickness with respect to the wall height and friction angle of the backfill material on the reduction in seismic earth pressure. Based on the results of this study, the following conclusions can been drawn:

1. The design of retaining structures supporting significant backfill in seismically active zones requires attention to the possible impact of dynamic loads on the earth pressure transferred to the retaining structure. Provision of EPS geofoam placed between the wall and backfill soil can help control the expected soil yield and mobilization of soil strength under dynamic loading. This in turn can lead to a reduction in the seismic thrust on the wall. An advantage of this technique is that it could be applied to both new and existing structures.
2. For the investigated wall and backfill material, the dynamic response of the backfill soil is reasonably predicted using the Hardening Soil model.

3. For the range of investigated parameters, the performance of EPS geofoam as seismic buffer is found to be function of the material density, relative thickness as well as the frictional properties of backfill soil.
4. It was confirmed that low density geofoam better absorbs seismic waves and provides enhanced performance. On the other hand, for a given geofoam density, increasing the thickness of the geofoam block is found to contribute to significant reduction in total thrust on the wall.
5. It is pointed out that geofoam inclusion used in this study had a relative thickness that ranges from 10 to 30% of the wall height. Although this is considered to be within the practical range, other wall geometries, backfill types and geofoam thicknesses need to be further investigated.

Acknowledgements The work presented in this paper is supported by McGill University, Canada and the University of Engineering and Technology, Lahore, Pakistan. Geofoam material data were provided by Plasti-Fab Inc., their contribution is really appreciated.

Author Contributions Analysis, writing original draft, MI. Khan; editing and reviewing, M.A. Meguid. All authors have read and agreed to the published version of the manuscript.

Funding Other than the graduate scholarship awarded to MI. Khan, this research received no external funding.

Data Availability The data that support the findings of this study are available on request from the corresponding author.

Declarations

Conflict of interest The authors declare no conflict of interest.

References

1. Horvath JS (1992) New developments in geosynthetics; 'lite' products come of age. Standardization News 20(9):50–53
2. Horvath JS (1995) Geofoam geosynthetic,. Horvath engineering, New York, p 217
3. Horvath JS (1991) The case of an additional function. IGS News 7(3):17–18
4. Aaboe R (2000) Evidence of EPS long term performance and durability as a lightweight fill. Vegteknisk avdeling
5. Frydenlund T (1991) Expanded polystyrene: a lighter way across soft ground, vol 1502. ICON Group International
6. Elragi AF (2000) Selected engineering properties and applications of EPS geofoam. ProQuest Dissertations and Theses
7. Jutkofsky W, Sung J, Negussey D (2000) Stabilization of embankment slope with geofoam. Transport Res Rec JTransport Res Board 1736:94–102
8. Sheeley M (2000) Slope stabilization utilizing geofoam. Master's thesis, Syracuse University, New York
9. Srirajan S (2001) Recycled content and creep performance of EPS geofoam in slope stabilization. Doctoral dissertation. Syracuse University, New York
10. Negussey D (2002) Slope stabilization with geofoam. Report to FHWA and the EPS industry. Geofoam research center, Syracuse University, New York
11. Stark TD, Arellano D, Horvath JS, Leshchinsky D (2004) Geofoam applications in the design and construction of highway embankments. NCHRP Web Doc 65:24–11
12. Duskov M (1991) Use of expanded polystyrene (EPS) in flexible pavements on poor subgrades. In: Proceedings of the International Conference on geotechnical engineering for coastal development, pp 783–788
13. Duskov M (1997) Measurements on a flexible pavement structure with an EPS geofoam sub-base. Geotext Geomembr 15(1):5–27. https://doi.org/10.1016/S0266-1144(97)00004-6
14. Riad HL, Ricci AL, Osborn PW, Horvath JS (2003) Expanded polystyrene (EPS) geofoam for road embankments and other lightweight fills in urban environments. In: Soil and Rock America, 12th Pan-American Conference on soil mechanics and geotechnical engineering and 39th US Rock Mechanics Symposium
15. Refsdal G (1985) Plastic foam in road embankments: future trends for EPS use. Internal report, Norwegian Road Research Laboratory, Oslo, Norway
16. Aaboe R (1987) 13 years of experience with expanded polystyrene as a lightweight fill material in road embankments. Nor Road Res Lab Publ 61:21–27
17. Zou Y, Leo C, Small J (2000) Behaviour of EPS geofoam as flexible pavement subgrade material in model tests. Geosynth Int 7(1):1–22
18. Negussey D, Stuedlein A, Bartlett S, Farnsworth C (2001) Performance of a geofoam embankment at 100 South, I-15 reconstruction project, Salt Lake City, Utah. In: Proceedings on 3rd International Conference on EPS Geofoam
19. Farnsworth C, Bartlett SF, Negussey D, Stuedlein A (2008) Rapid construction and settlement behavior of embankment systems on soft foundation soils. J Geotech Geo-Environ Engg 134(3):289–301
20. Frydenlund T, Aaboe R (1996) Expanded polystyrene-the light solution. In: Proceedings of international symposium on EPS construction method (EPS-Tokyo'96), Tokyo, Japan, pp 31–46
21. Williams, D.; Snowdon, R. (1990) A 47 Great Yarmouth Western Bypass: Performance during the First Three Years (No. 11); Transport and Road Research Laboratory (TRRL): Berkshire, UK, 1990
22. Skuggedal H, Aaboe R (1991) Temporary overpass bridge founded on expanded polystyrene. In: Proceedings of the 1st European conference on soil mechanics and foundation engineering, pp 559–561
23. McDonald P, Brown P (1993) Ultra lightweight polystyrene for bridge approach fill. In: Proceedings of the 11th Southeast Asian geotechnical conference, Singapore, pp 664–668
24. Bang S (1995) Experimental and analytical study of expanded polystyrene blocks in highway application. In: Proceedings of international seminar on the application of EPS for embankment construction, Korea Institute of Construction Technology (KICT), Seoul, Korea, pp 105–133
25. Abu-Hejleh N, Zornberg JG, Elias V, Watcharamonthein J (2003) Design assessment of the founders/meadows GRS abutment structure. In: Proceedings of 82nd annual TRB meeting
26. Meguid M, Ahmed M, Hussein M, Omeman Z (2017) Earth pressure distribution on a rigid box covered with u-shaped geofoam wrap. Int J Geosyn Ground Eng 3(2):11
27. Meguid M, Hussein M (2017) A numerical procedure for the assessment of contact pressures on buried structures overlain by EPS geofoam inclusion. Int J Geosyn Ground Eng 3(1):2
28. Meguid M, Hussein M, Ahmed M, Omeman Z, Whalen J (2017) Investigation of soil-geosynthetic-structure interaction

associated with induced trench installation. Geotext Geomembr 45(4):320–330
29. Zarnani S, Bathurst R (2007) Experimental investigation of EPS geofoam seismic buffers using shaking table tests. Geosynth Int 14(3):165–177
30. Horvath JS (1997) The compressible inclusion function of EPS geofoam. Geotext Geomembr 15(1):77–120
31. Bathurst RJ, Keshavarz A, Zarnani S, Take WA (2007) A simple displacement model for response analysis of EPS geofoam seismic buffers. Soil Dyn Earthq Eng 27(4):344–353
32. Ossa A, Romo M (2011) Dynamic characterization of EPS geofoam. Geotext Geomembr 29(1):40–50
33. Partos A, Kazaniwsky P (1987) Geoboard reduces lateral earth pressures. In: Proceedings of geosynthetics' 87 conference, New Orleans, USA, pp 628–639
34. Horvath JS (2010) Lateral pressure reduction on earth-retaining structures using geofoams: correcting some misunderstandings. In: Earth retention conference, pp 862–869
35. Koseki J, Bathurst RJ, Guler E, Kuwano J, Maugeri M (2006) Seismic stability of reinforced soil walls. In: Paper presented at the 8th international conference on geosynthetics, Yokohama, Japan, September 2006, pp 18–22
36. AASHTO (2010) American Association of State Highway and Transportation Officials LRFD bridge design specifications, 5th edn. AASHTO, Washington, DC
37. NBCC (2010) National Building Code of Canada. National Research Council of Canada, Ottawa
38. Inglis D, Macleod G, Naesgaard E, Zergoun M (1996) Basement wall with seismic earth pressures and novel expanded polystyrene foam buffer layer. In: Paper presented at the 10th annual symposium on Earth retention system, Vancouver, Canada
39. Gaskin AP (2000) Geofoam buffers for rigid walls: An investigation into the use of expanded polystyrene for seismic buffers. Master's Thesis, Queen's University, Kingston, Canada
40. Hazarika H, Okuzono S, Matsuo Y (2003) Compressible geo-inclusion as a seismic earth pressure reduction technique. In: Paper presented at the 38th Japan National conference on geotechnical engineering
41. Athanasopoulos GA, Nikolopoulou CP, Xenaki VC, Stathopoulou VD (2007) Reducing the seismic earth pressure on retaining walls by EPS geofoam buffers—numerical parametric study. In: Paper presented at the geosynthetics conference, Washington DC, USA
42. Bathurst RJ, Zarnani S, Gaskin A (2007) Shaking table testing of geofoam seismic buffers. Soil Dyn Earthq Eng 27(4):324–332. https://doi.org/10.1016/j.soildyn.2006.08.003
43. Athanasopoulos-Zekkos A, Lamote K, Athanasopoulos G (2011) Seismic isolation of earth retaining walls using EPS compressible inclusions—results from centrifuge testing. In: Paper presented at the 4th international conference on geofoam blocks in construction applications, Lillestrøm, Norway
44. Dasaka SM, Dave TN, Gade VK, Chauhan VB (2014) Seismic earth pressure reduction on gravity retaining walls using eps geofoam. In: Paper presented at the 8th international conference on physical modelling in geotechnical engineering, Perth, Australia
45. Ertugrul OL, Trandafir AC (2014) Seismic earth pressures on flexible cantilever retaining walls with deformable inclusions. J Rock Mech Geotech Eng 6(5):417–427. https://doi.org/10.1016/j.jrmge.2014.07.004
46. Partos A, Kazaniwsky P (1987) Geoboard reduces lateral earth pressures. In: Proceedings of geosynthetics, pp 628–639
47. McGown A, Andrawes KZ, Murray RT (1988) Controlled yielding of the lateral boundaries of soil retaining structures. In: Symposium on geosynthetics for soil improvement at the ASCE convention. vol Geotechnical Special
48. Karpurapu R, Bathurst R (1992) Numerical investigation of controlled yielding of soil-retaining wall structures. Geotext Geomembr 11(2):115–131
49. Horvath JS (2004) Geofoam compressible inclusions: the new frontier in earth retaining structures. In: Geotechnical engineering for transportation projects, pp 1925–1934
50. Lutenegger AJ, Ciufetti M (2009) Full-scale pilot study to reduce lateral stresses in retaining structures using geofoam. Final report, project No RSCH010–983 Vermont DOT, University of Massachusetts, Amherst, MA
51. Ertugrul OL, Trandafir AC (2011) Reduction of lateral earth forces acting on rigid nonyielding retaining walls by EPS geofoam inclusions. J Mater Civ Eng 23(12):1711–1718
52. Athanasopoulos-Zekkos A, Lamote K, Athanasopoulos G (2012) Use of EPS geofoam compressible inclusions for reducing the earthquake effects on yielding earth retaining structures. Soil Dyn Earthq Eng 41:59–71
53. McGown A, Murray R, Andrawes K (1987) Influence of wall yielding on lateral stresses in unreinforced and reinforced fills. Research Report 113, Transportation and Road Research Laboratory, Crowthorne, Berkshire, UK
54. Khan MI, Meguid MA (2021) Evaluating the role of geofoam properties in reducing lateral loads on retaining walls: a numerical study. Sustainability 13(9):4754
55. Inglis D, Macleod G, Naesgaard E, Zergoun M (1996) Basement wall with seismic earth pressures and novel expanded polystyrene foam buffer layer. In: Proceedings of the 10th annual symposium of the Vancouver geotechnical society, Vancouver, BC
56. Sarma SK (1973) Stability Analysis of Embankments and Slopes. Geotechnique 23(3):423–433
57. Byrne PM, Jitno H, Salgado F (1992) Earthquake induced displacements of soil-structures systems. In: Proceedings of 10th World conference on earthquake engineering, pp 1407–1412
58. Jitno H, Byrne PM (1994) (1994) A procedure for predicting seismic deformation of earth structures. Vertical and horizontal deformations of foundations and embankments. ASCE, pp 711–725
59. Byrne PM, Janzen W (1981) Soil stress: a computer program for nonlinear analysis of stresses and deformations in soils. Department of Civil Engineering, University of British Columbia
60. Cundall P, Board M (1988) A microcomputer program for modelling large-strain plasticity problems. In: Proceedings of the sixth international conference on numerical methods in geomechanics, vol1–3. Innsbruck, Austria, 11–15 April 1988
61. Hazarika H, Okuzono S, Matsuo Y (2003) Seismic stability enhancement of rigid nonyielding structures. In: Paper presented at the 13th international offshore and polar engineering conference, Honolulu, Hawaii, USA
62. Dave TN, Dasaka SM (2015) Effect of boundary conditions on earth pressure reduction using eps geofoam. In: Paper presented at the 15th Asian Regional Conference on Soil Mechanics and Geotechnical Engineering, Fukuoka, Japan
63. Ertugrul OL, Trandafir AC (2012) A physical modeling study on the dynamic response of flexible retaining walls with deformable EPS inclusion. In: Paper presented at the 15th World Conference on Earthquake Engineering, Lisbon, Portugal
64. Ertugrul OL, Trandafir AC, Ozkan MY (2017) Reduction of dynamic earth loads on flexible cantilever retaining walls by deformable geofoam panels. Soil Dyn Earthq Eng 92(20):462–471. https://doi.org/10.1016/j.soildyn.2016.10.011
65. Pelekis P, Xenaki V, Athanasopoulos G (2000) Use of EPS geofoam for seismic isolation of earth retaining structures: Results of

a FEM study. In: Proceedings of the 2nd European geosynthetics conference, Bologna, Italy, pp 15–18
66. Armstrong R, Alfaro M (2003) Reduction of seismic-induced pressures on rigid retaining structures using compressible inclusions: a numerical study. In: Proceedings of the 56th Canadian geotechnical conference, Winnipeg, Man, pp 500–505
67. Zarnani S, Bathurst RJ (2008) Numerical modeling of EPS seismic buffer shaking table tests. Geotext Geomembr 26(5):371–383. https://doi.org/10.1016/j.geotexmem.2008.02.004
68. Zarnani S, Bathurst RJ (2005) Numerical Investigation of geofoam seismic buffers using FLAC. In: Paper presented at the North American geosynthetics society (NAGS)/GR119 conference, Las Vegas, NV, USA
69. Zarnani S, Bathurst R (2010) Numerical parametric study of geofoam seismic buffers with different constitutive models. In: Proceedings of the 9th international geosynthetics conference, 2010, pp 1665–1668
70. Zarnani S, Bathurst RJ (2009) Numerical parametric study of expanded polystyrene (EPS) geofoam seismic buffers. Can Geotech J 46(3):318–338. https://doi.org/10.1139/T08-128
71. Athanasopoulos G, Nikolopoulou C, Xenaki V, Stathopoulou V (2007) Reducing the seismic earth pressures on retaining walls by EPS geofoam buffers—numerical parametric analyses. In: Proceeding of geosynthetics
72. Zekkos AA, Lamote K, Athanasopoulos GA (2012) Use of EPS geofoam compressible inclusions for reducing the earthquake effects on yielding earth retaining structures. Soil Dyn Earthq Eng 41:59–71. https://doi.org/10.1016/j.soildyn.2012.05.004
73. Wang YM, Li H, Zhang H (2012) Numerical simulation for dynamic response of EPS geofoam seismic buffers. Adv Mater Res 378:256–261
74. Wang D, Bathurst RJ (2012) Numerical analysis of earthquake load mitigation on rigid retaining walls using EPS geofoam. Open Civ Eng J 6:21–25
75. Iai S (1989) Similitude for shaking table tests on soil-structure-fluid model in 1g gravitational field. Soils Found 29(1):105–118
76. Bathurst RJ, Hatami K (1998) Seismic response analysis of a geosynthetic-reinforced soil retaining wall. Geosynth Int 5(1–2):127–166. https://doi.org/10.1680/gein.5.0117
77. Matsuo O, Yokoyama K, Saito Y (1998) Shaking table tests and analyses of geosynthetic-reinforced soil retaining walls. Geosynth Int 5(1–2):97–126
78. Brinkgreve R, Kumarswamy S, Swolfs W, Waterman D, Chesaru A, Bonnier P (2020) PLAXIS 2D Version 20.03.00.60. Netherlands
79. Schanz T (1999) Formulation and verification of the Hardening-Soil model. In: RBJ Brinkgreve, beyond 2000 in computational geotechnics, pp 281–290